T-2317

AN ITERATIVE SEISMIC RAY-MIGRATION SCHEME FOR COMPLEX STRUCTURES

by

Robert W. Wiley

A thesis submitted to the Faculty and the Board of Trustees of the Colorado School of Mines in partial fulfillment of the requirements for the degree of Doctor of Philosophy in Geophysics.

Golden, Colorado

Date 25 April, 1980

Signed: Robert W. Wiley
Robert W. Wiley

Approved: Frank A. Hadsell
Frank A. Hadsell
Thesis Advisor 25 apr 80

Golden, Colorado
Date 4/25, 1980

P R Romig
Head of Department

ABSTRACT

A method for determining interval velocity and subsurface location of geologic layers of arbitrary shape is presented. The method uses offset raytracing and inverse normal incident raytracing in order to develop a geologic cross section. By blending these two forms of raytracing, it is possible to maintain the accuracy of least-squares iteration schemes while greatly reducing the computer time. Travel time, stacking velocities, and the CDP configuration are the only parameters needed for this approach.

A synthetic example using a model from a geologic overthrust region demonstrates the quality of the solution. The model points out the flexibility of the method as it contains velocity inversions, sharply curved interfaces, and beds which terminate laterally. Because of the time required to run the example, this method is recommended only for those areas where other techniques for estimating velocity and depth fail.

TABLE OF CONTENTS

LIST OF FIGURES AND TABLES

Page

ACKNOWLEDGEMENT

The author would like to thank Marathon Oil Company for providing the data and for their generosity in the use of their computer.

INTRODUCTION

Because of the increasing importance of lithologic interpretation of seismic data the geophysicist has an ever greater need for accurate interval velocity information. In areas of complex subsurface geology, this interval velocity information is often difficult if not impossible to obtain without well control. This difficulty is caused by dip, curvature of the interfaces, lateral changes in velocity, and lateral termination of beds.

There are several approaches for handling the problem of dip. Some methods use a simple cosine correction (Levin 1971, Everett 1974) to the interval velocity calculated from Dix's formula (Dix 1955). These methods provide a satisfactory answer in a uniformly dipping sequence. However they cannot handle a sequence of varying dips. Other approaches use least squares techniques and raytracing (Sattleger 1965) to iteratively improve estimates of interval velocity, dip, and depth. While the results of this approach are quite satisfactory, the method uses large amounts of computer time and requires high quality picks of reflection time on each individual trace. A third approach, the analytic method, uses closed form expressions (Larner 1972) which directly yield interval velocity, dip and depth of dipping layered media. This technique is both fast and accurate, but the equations only hold for planar or moderately curved interfaces. Thus it cannot handle problems encountered in a region like the overthrust belt of western Wyoming where there are both tight curves and beds which terminate laterally.

The approach presented in this paper is a combination of the analytic method and the scheme employing offset raytracing. In this way, I can get the accuracy and generality of Sattleger's raytracing technique and yet avoid the large amounts of computer time. With the accuracy and generality of the raytracing approach, this method will work in those areas of complex geology where analytical techniques such as Larner's fail.

DIFFICULTIES WITH VELOCITIES

The cross section in Figure 1 is a model of the overthrust belt of western Wyoming. This cross section, which is typical of the overthrust region, contains layers with varying dips, sharp curvatures, as well as a complex of beds which truncate laterally. This cross section was developed by R. M. Bone of Marathon Oil Company using a combination of seismic data well logs.

The Common Depth Point Gather

Figure 2 is the outlined portion of Figure 1. Here the raypaths for a sixfold "common depth point" (CDP) gather reflecting off the tenth interface are drawn in. Of course, with these dipping layers, no true common depth point exists. However, even in this model, all of the reflection points along a horizon for a given CDP gather usually fall within one Fresnel zone of the reflection point of the normal incident raypath.

In Figure 2, the raypaths for the far traces pass through a low velocity wedge which is above the third interface. However the near traces do not. This low velocity wedge will cause the calculated stacking velocity to be slower than the stacking velocity derived from the normal incident raypath. Dix, however, in his interval velocity

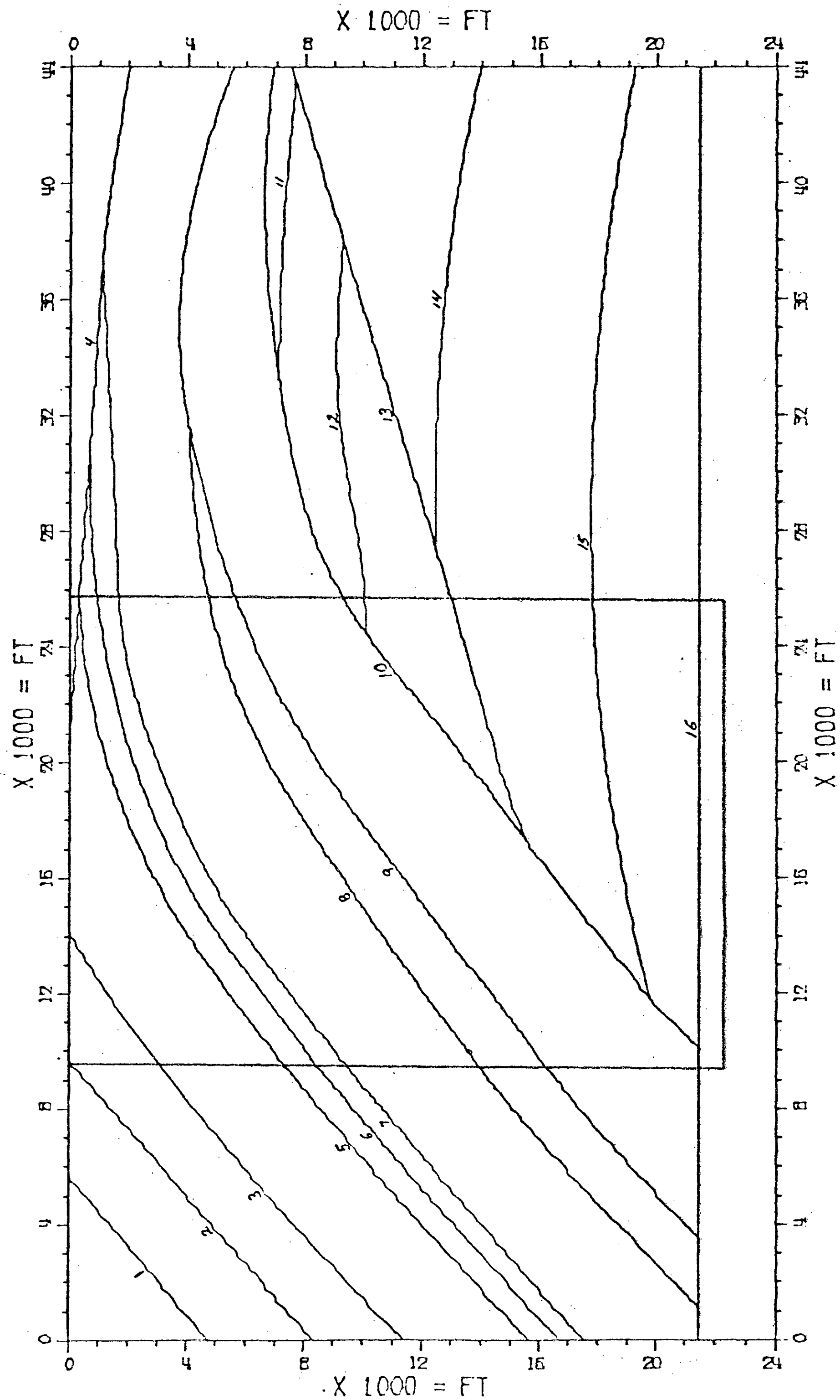

A Geologic Cross Section of the Overthrust Belt

(Developed by R. M. Bone, Marathon Oil Co.)

FIGURE 1

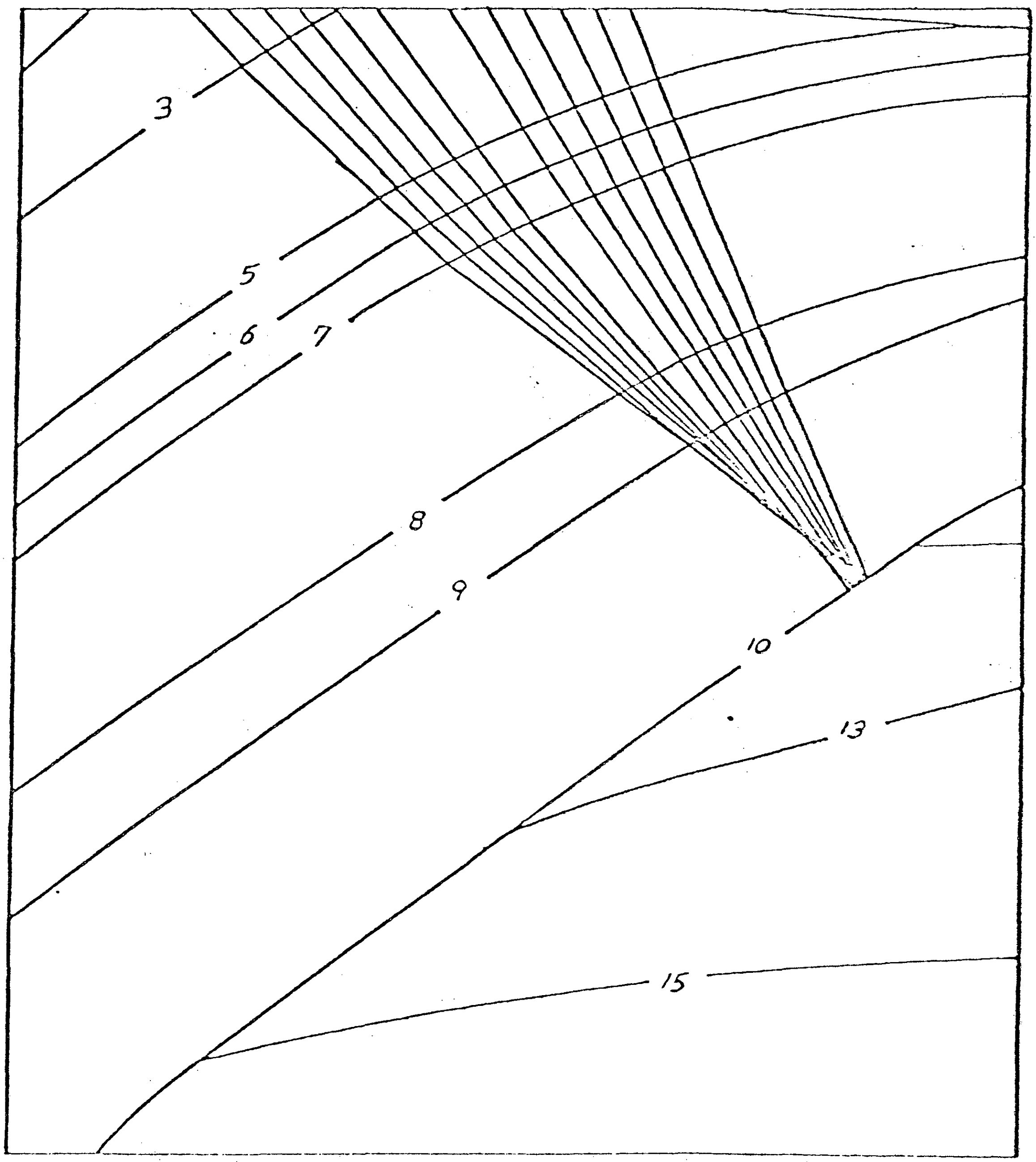

Reflection Paths for a Selected 6 Fold Gather Reflecting Off of the Tenth Interface (Outlined Portion of Figure 1)

FIGURE 2

equation, assumes that the RMS or stacking velocity which is used is the normal incident or zero offset stacking velocity. This then will cause an error in the interval velocities which are derived from the slower stacking velocity.

Non-Alignment of Reflection Points

The major problem in determining interval velocity is depicted in Figure 3. This figure is the same portion of the model as is shown in Figure 2. Here, however, the zero offset or normal incident raypaths for a number of reflection horizons of the CDP have been drawn in. It is obvious that the reflecting points on the various interfaces are not aligned vertically, nor in any other fashion. Because of this lack of order in the reflecting points, the interval velocities for layers 1 through 9, for example, cannot be directly used to determine the interval velocity for layer 10. This is further illustrated in Figure 6. Figure 6 is a plot of the velocity analysis obtained from the gather in Figure 5. The interpretation of the stacking velocity has been made and is the dashed line on Figure 6. Interval velocities were then calculated using Dix formula and plotted with a solid line. No attempt was made to correct for dip. In the plot of the interval velocities there is a gap that contains a question mark. This interval has an interval velocity that is imaginary when Dix's formula is used. This

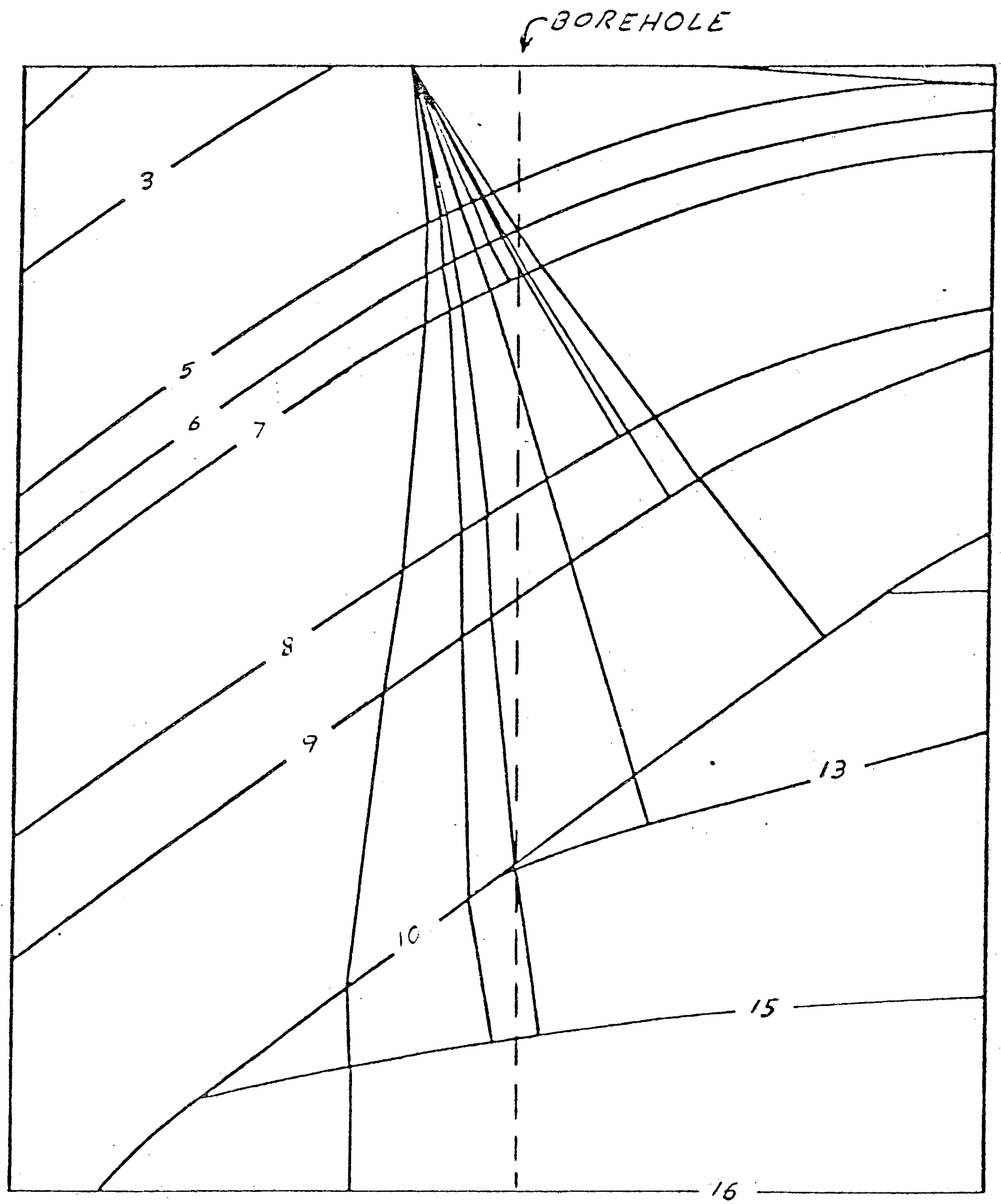

Zero Offset Reflection Paths for a Single CDP

(Outlined Portion of Figure 1)

FIGURE 3

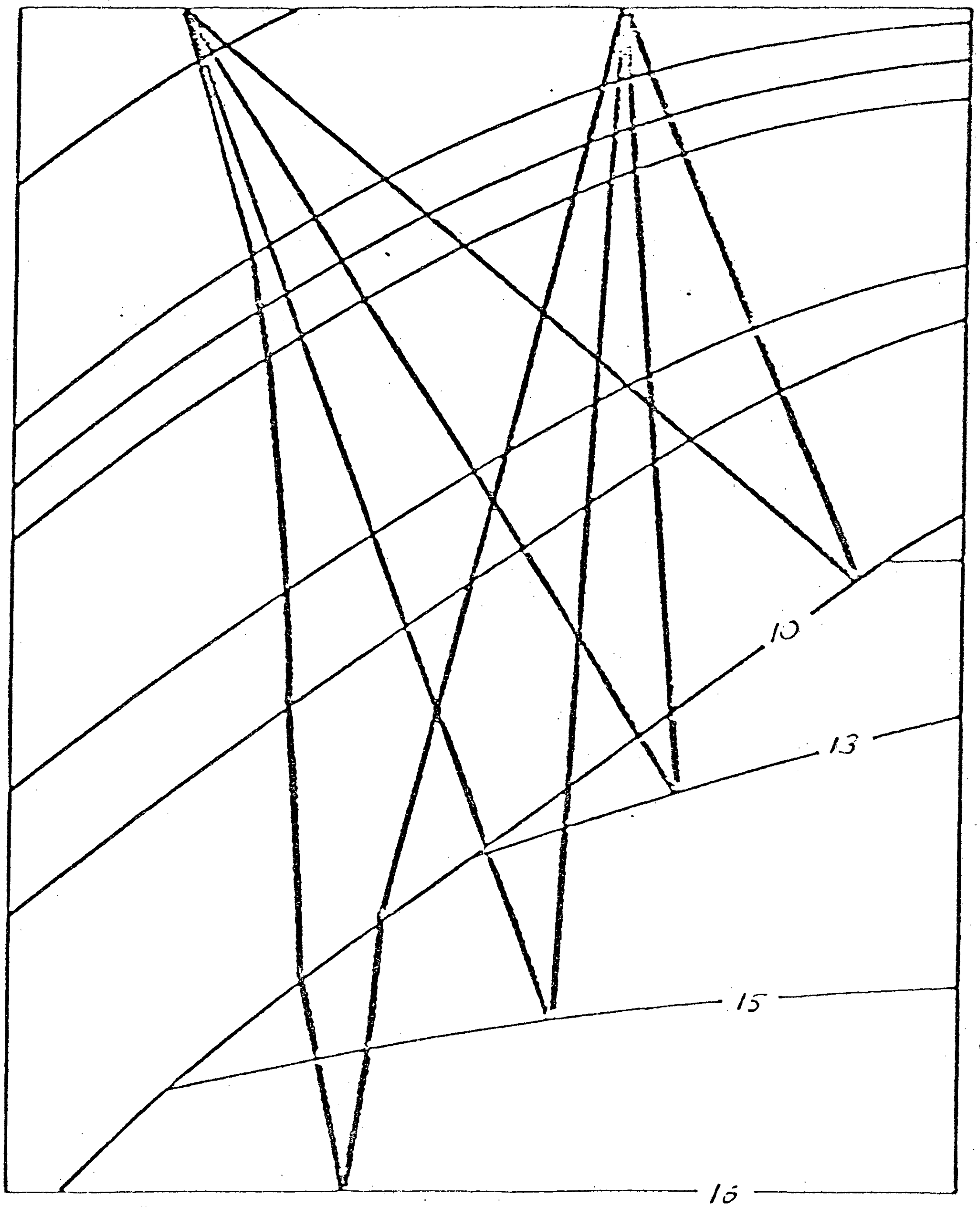

Far Offset Reflection Paths for a Single CDP

(Outlined Portion of Figure 1)

FIGURE 4

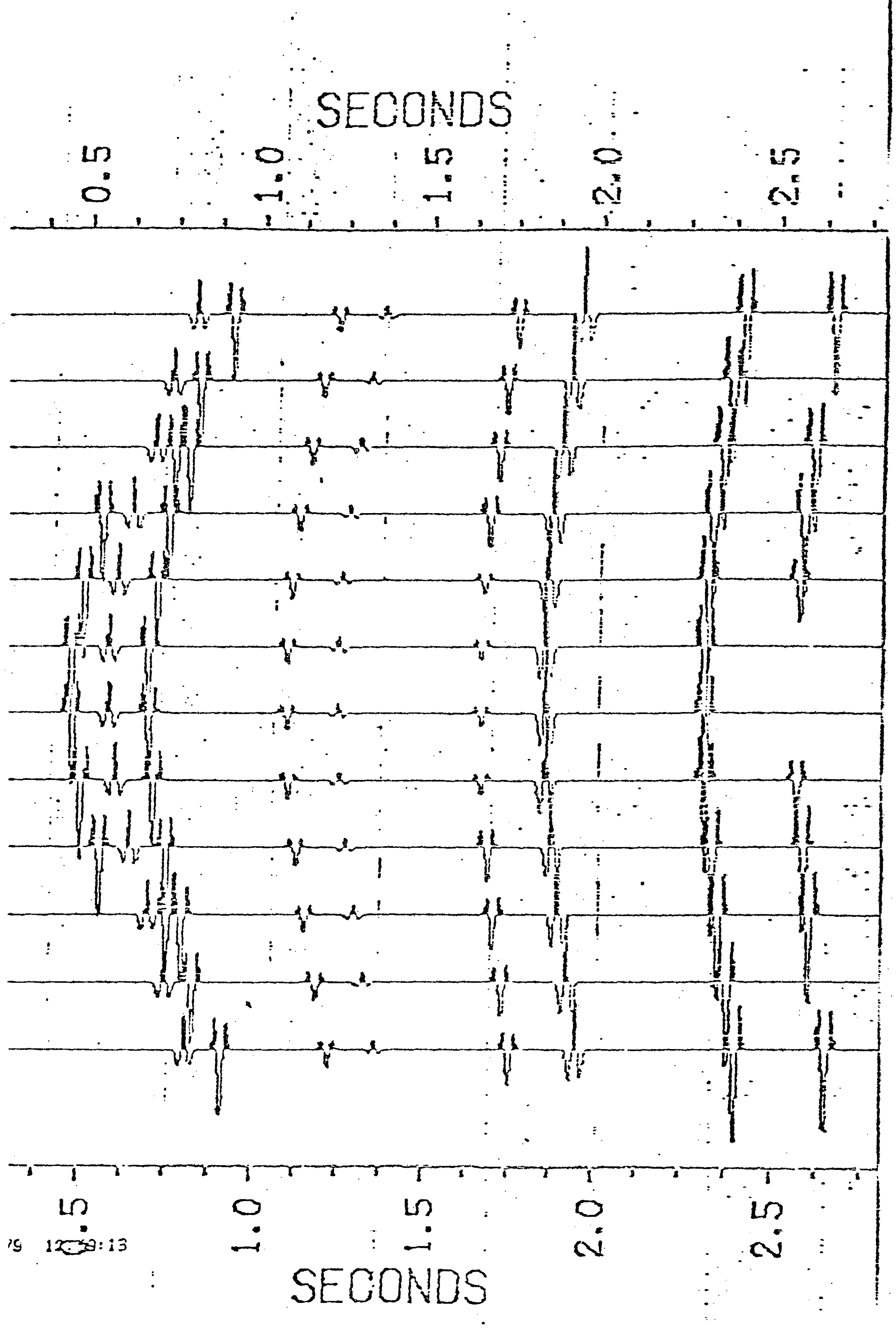

Plot of All Reflections for the Gather from Figure 2

FIGURE 5

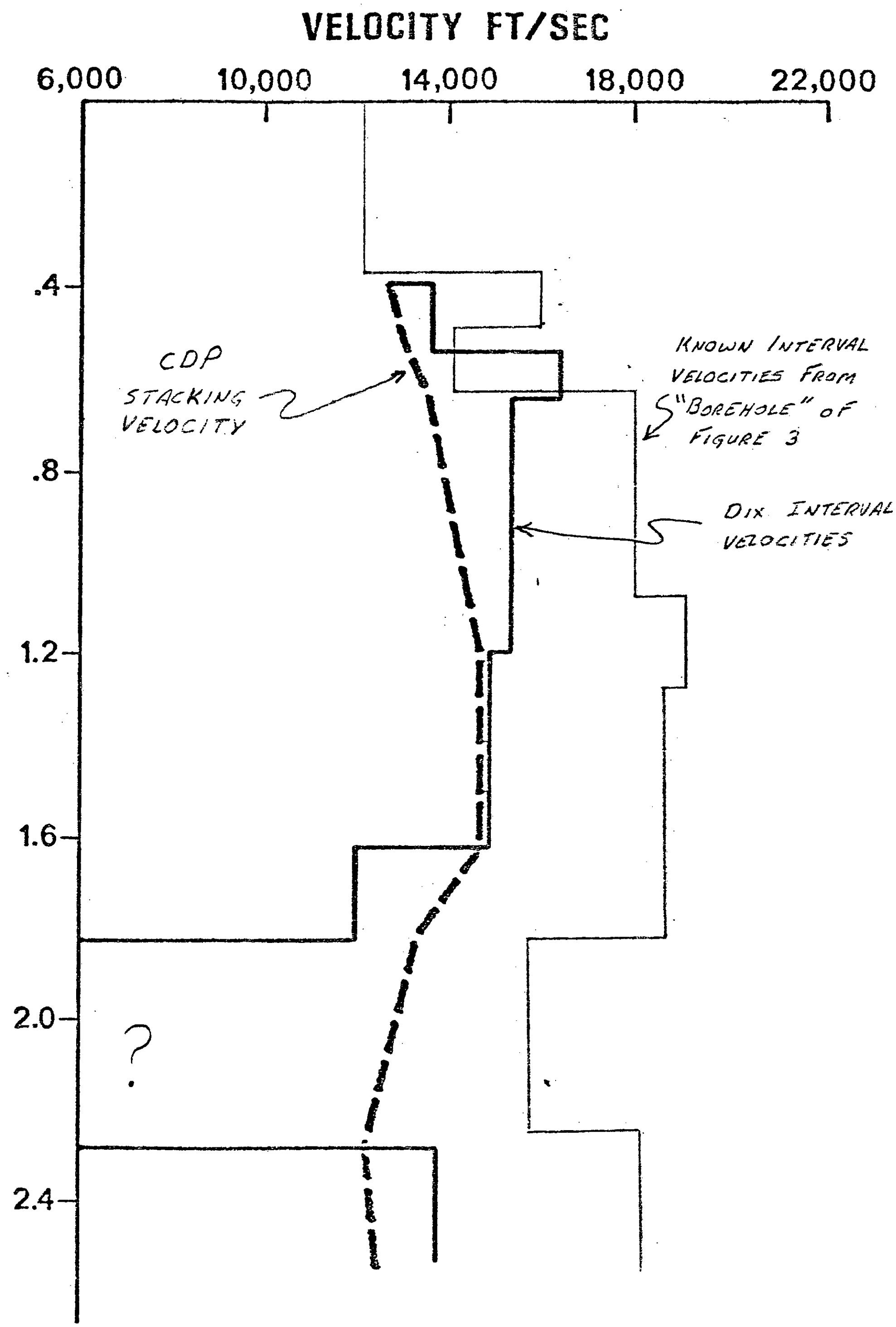

CDP Velocity Analysis at Borehole in Figure 3

FIGURE 6

imaginary velocity means that Dix's formula will not work in structurally complex areas where the reflecting points are not aligned. Since Levin's dip correction term is just a cosine correction applied to the Dix formula, Levin's dip correction will not work in these areas either. It is therefore necessary to find a new approach in order to determine interval velocities in structurally complex areas.

AN ALGORITHM FOR DETERMINING DEPTH

This paper presents a method for determining interval velocities, dip, and depth in structurally complex areas. This approach uses a velocity estimation technique to establish a first approximation of the interval velocity. Then the method iterates between a method for determining depth and dip and a method for updating the interval velocity. The velocity estimation technique comes from the work of Durbaum (1954). The method for correcting the interval velocity is based on Sattleger (1965) and the means of determining depth and dip is based on Durbaum (1953).

The complete method for determining depth, dip, and interval velocity in structurally complex areas as presented in this paper is shown in Figure 7. This figure is a computer flow chart and merges the three partial methods, depth and dip determination, velocity estimation, and velocity correction into one uniform approach. Symbols used in this chart are defined on pages 17, 18, 27, and 30. The flow chart has been broken into three connected segments in order to categorize the various aspects of the method. Figure 7a contains the setup of the model parameters and the seismic shooting pattern. The input of the seismic data, the time picks and the stacking velocities, is contained in this block. Also contained in this block is the input of any knowledge of

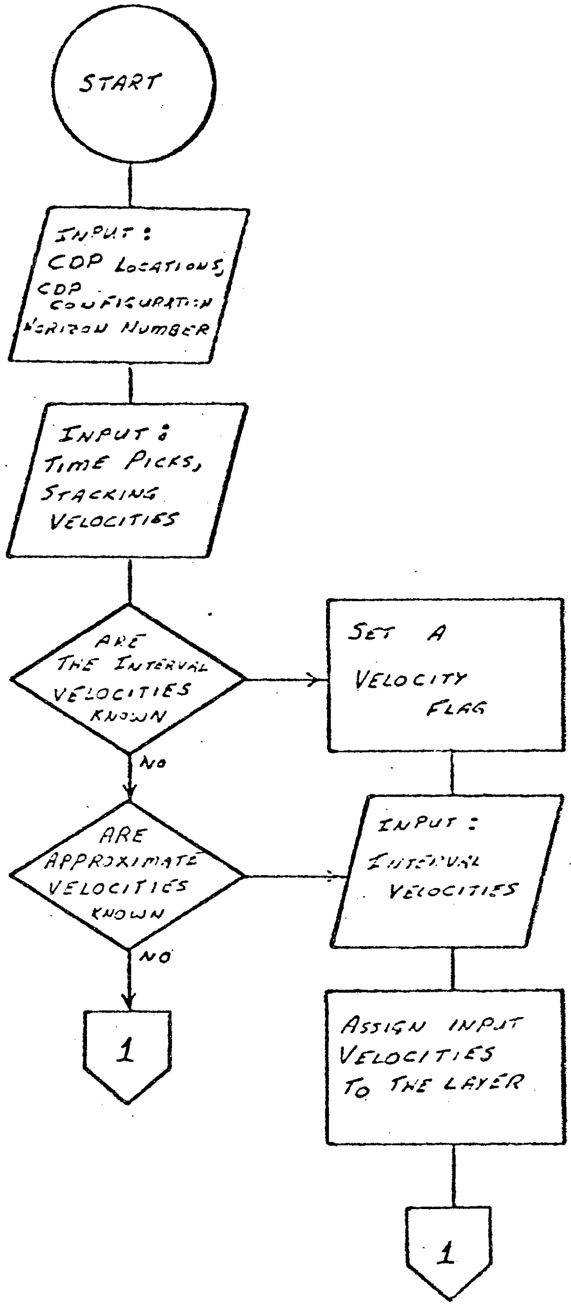

Computer Flow Chart for Inputting Data

FIGURE 7a

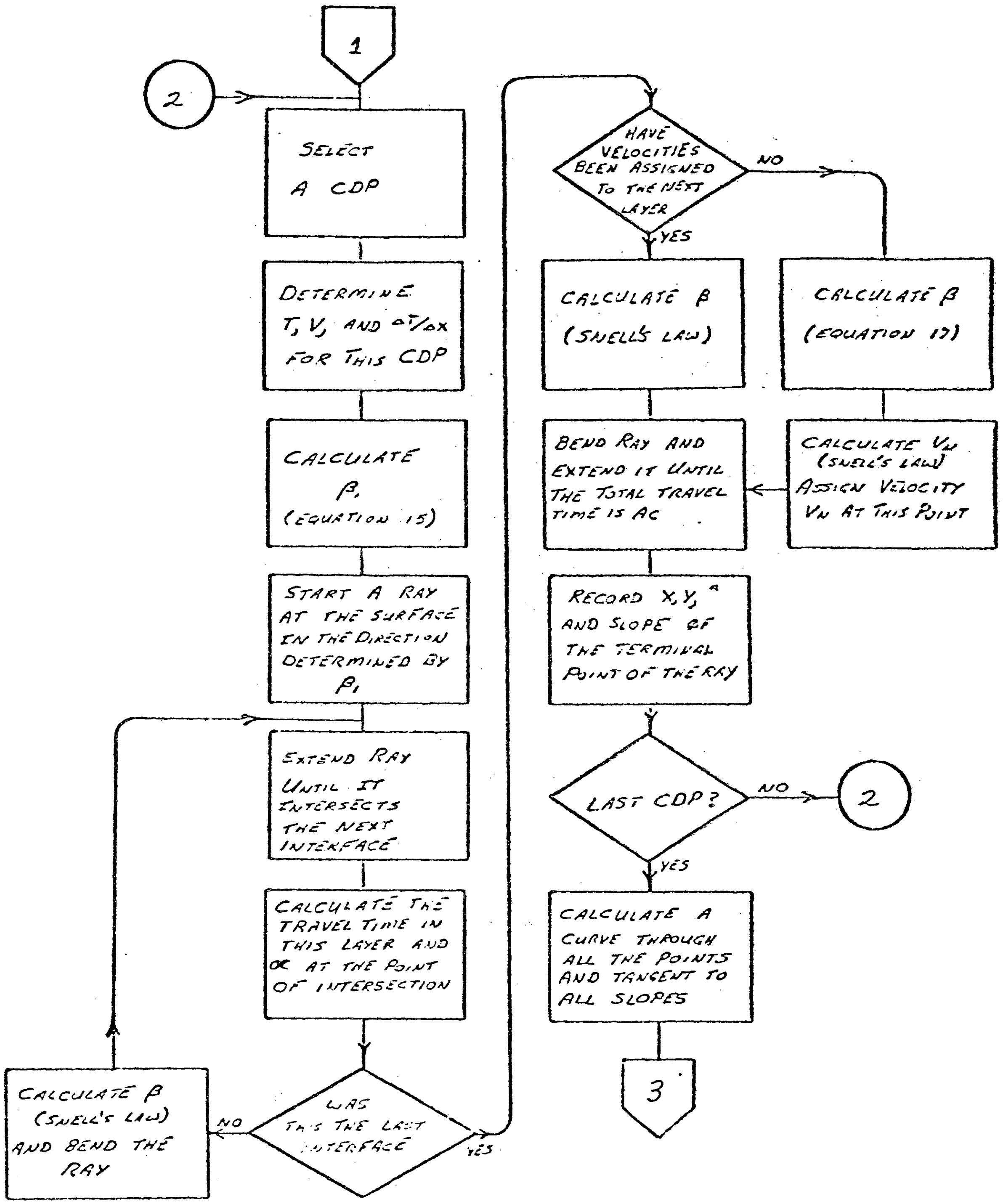

Flow Chart for Determining Depths

FIGURE 7b

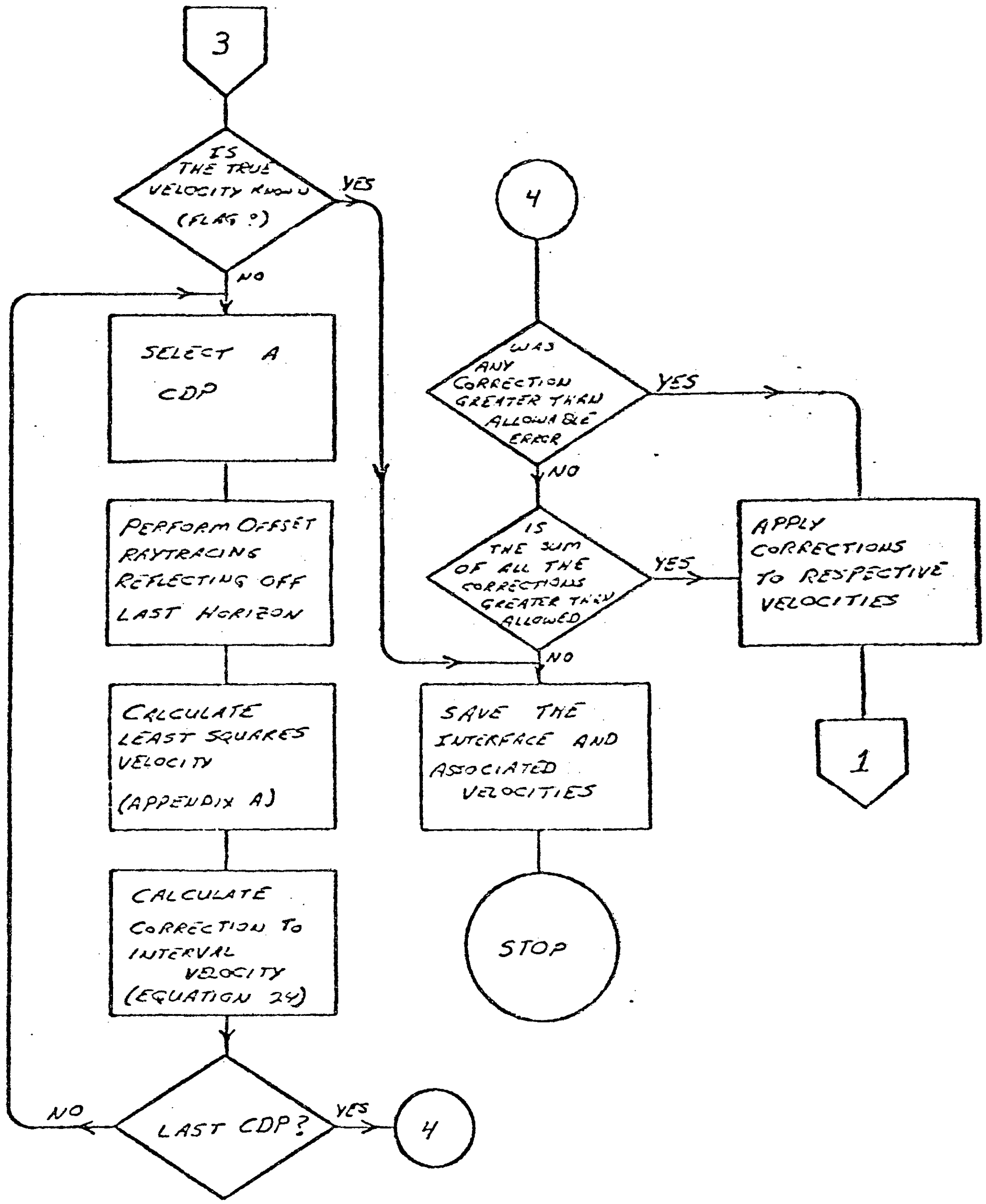

Flow Chart for Calculating Velocity

FIGURE 7c

the interval velocities. In Figure 7b, an estimate of the interval velocity is calculated if none exists. Also the location of the interface is determined using the estimated interval velocity. Figure 7c includes the calculation of the correction to the interval velocity. Storing the results is handled by Figure 7c if no correction is made to the interval velocity. Using this flow chart, it is possible to write a computer program which will use the methods outlined in this paper to calculate both interval velocities and depths.

DEPTH AND DIP DETERMINATION

In order to simplify the calculations, it was necessary to separate depth and dip from the calculation for interval velocity. This was done using the concept of time dip which was developed by Durbaum in 1953. With this concept from Durbaum it is possible to express both depth and dip as functions of velocity, thus eliminating two of the variables. The following is a proof of the two-dimensional time dip equation adapted from Durbaum's three-dimensional proof.

Notation

The following notation will be used in the proof:

interface i $\equiv$ interface between layer i and layer i + 1

x_k $\equiv$ location of kth shotpoint-geophone pair

raypath k $\equiv$ the raypath which intersects the free surface at x_k and is perpendicular to interface n (interface n is the interface for which the depth is to be determined). Since n is assumed to be fixed for this proof, the interface index will be suppressed.

v_i $\equiv$ interval velocity of layer i

$t_{k,i}$ $\equiv$ travel time in layer i measured along raypath k

$\Delta t_i \equiv t_{k+1,i} - t_{k,i}$, where raypath k+1 is the raypath nearest to but to the right of raypath k. Henceforth on this proof only one pair of rays will be considered, the first and second (k=1 and 2)

$T_i = \sum_{j=i}^{n} \Delta t_j$

$\theta_i \equiv$ dip of interface i (see Figure 8) ($i \leq n$)

$\phi_i = \theta_{i+1} - \theta_i$

$\alpha_i \equiv$ the angle of refraction of the upgoing raypath after penetrating interface i (see Figure 8)

$\beta_i \equiv$ the angle of incidence of the upgoing raypath and the normal to interface i (see Figure 8)

$\gamma_i = \Pi/2-\beta_i$ (see Figure 9b)

$\delta_i = \Pi-\gamma_i-\phi_i = \Pi - (\Pi/2-\beta_i) - \phi_i = \Pi/2 - (\phi_i-\beta_i)$ (see Figure 9b)

$q_i \equiv$ the distance between raypath 1 and raypath 2 measured along interface i

$l_{k,i} \equiv$ the length of raypath k which is in layer i (see Figure 9a)

Time Dip Equation

In the following proof, x_1 and x_2 are assumed to be sufficiently close that each interface is linear over the interval between the two raypaths. Since at both surface locations, x_1 and x_2, the shotpoint and geophone are together,

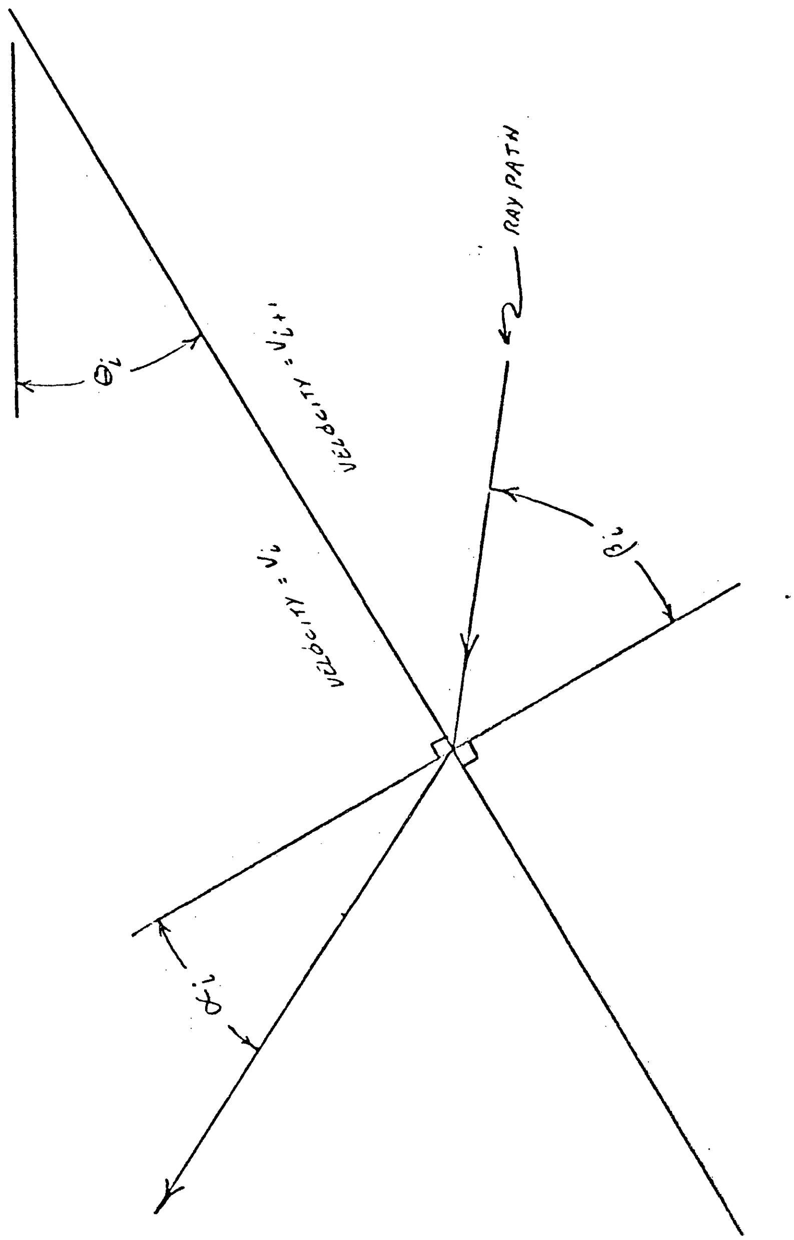

Travel Path Through a Single Interface

FIGURE 8

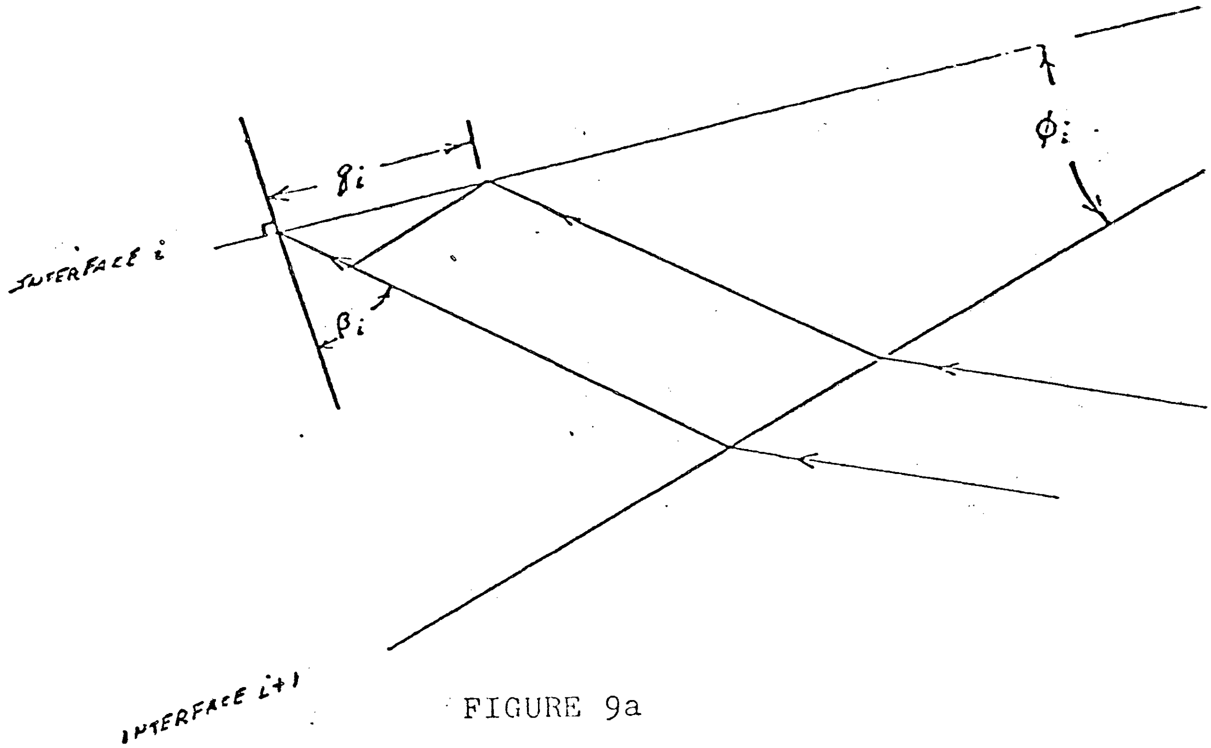

FIGURE 9a

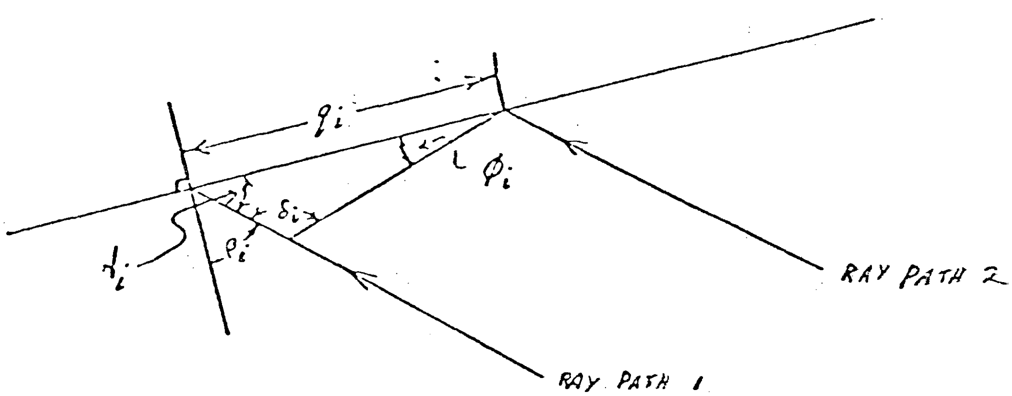

Parallel Travel Paths Through Two Interfaces

FIGURE 9b

it will only be necessary to consider the normal incident raypath.

Since the purpose is to express the time dip, $2T_1/(x_2-x_1)$, at the free surface as a function of the angle of incidence at the free surface, it is best to start at the reflecting horizon, interface n, and work upward. The normal incident raypaths are plotted in Figure 10, starting at the nth interface and intersecting the (n-1)th interface. The difference in travel time for the two raypaths through layer n is expressed as

$$t_{2,n}-t_{1,n} = 2(\ell_{2,n}/V_n-\ell_{1,n}/V_n) - 2(\ell_{2,n}-\ell_{1,n})/V_n \qquad (9)$$

However,

$$\ell_{2,i}-\ell_{1,i} = q_i \sin \beta_{n-1} .$$

Therefore

$$t_{2,n}-t_{1,n} = 2(q_{n-1} \sin \beta_{n-1})/V_n$$

or

$$1/2\Delta t_n = 1/2(t_{2,n}-t_{1,n}) = \frac{q_{n-1}}{V_n} \sin \beta_{n-1}$$

and therefore

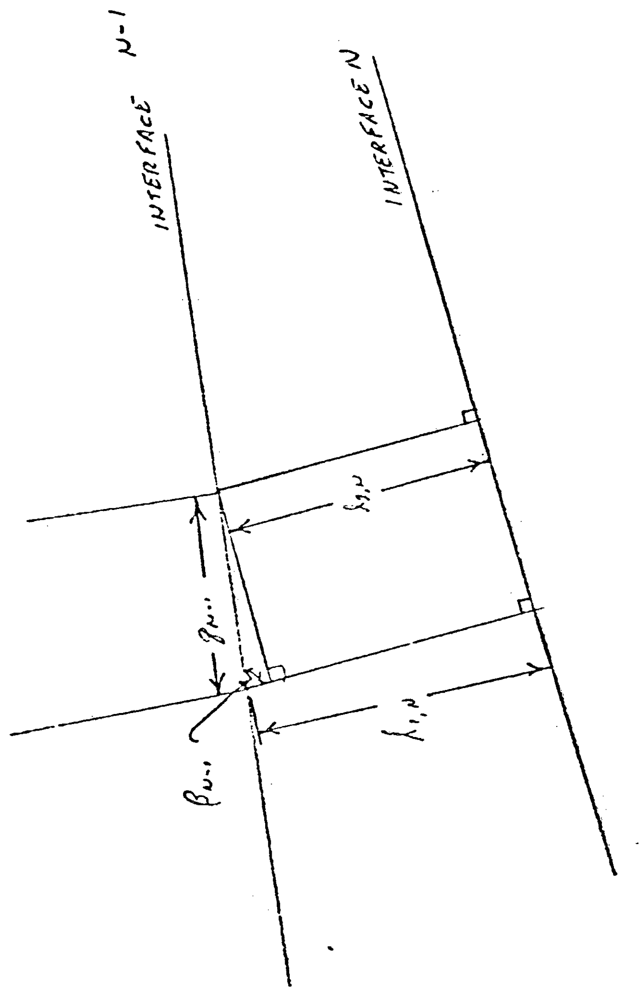

Normal Incident Raypaths Starting at Interface N

FIGURE 10

$$T_n/2 = 1/2\Delta t_n = \frac{q_{n-1}}{V_n} \sin \beta_{n-1} . \tag{10}$$

For the (n-1)th layer, shown in Figure 10

$$t_{2,n-1}-t_{1,n-1} = 2(\ell_{2,n-1}-\ell_{1,n-1})/V_{n-1}$$

and

$$\ell_{2,n-1}-\ell_{1,n-1} = q_{n-2} \sin \phi_{n-2}/\sin \delta_{n-2} .$$

Thus

$$1/2\Delta t_{n-1} = 1/2(t_{2,n-1}-t_{1,n-1}) = \frac{q_{n-2}}{V_{n-1}} \cdot \frac{\sin \phi_{n-2}}{\sin \delta_{n-2}}$$

and

$$T_{n-1}/2 = 1/2\Delta t_{n-1}+1/2\Delta t_n = \frac{q_{n-2}}{V_{n-1}} \frac{\sin \phi_{n-2}}{\sin \delta_{n-2}} + \frac{q_{n-1}}{V_n} \sin \beta_{n-1} . \tag{11}$$

Using the law of sines and Figure 9b

$$\frac{q_{n-2}}{\sin \delta_{n-2}} = \frac{q_{n-1}}{\sin \gamma_{n-2}}$$

or

$$q_{n-1} = q_{n-2} \frac{\sin \gamma_{n-2}}{\sin \delta_{n-2}} . \tag{12}$$

Putting this into equation 11 yields

$$T_{n-1}/2 = \frac{q_{n-1}}{V_n} \cdot \frac{\sin \phi_{n-2}}{\sin \delta_{n-2}} + \frac{q_{n-2}}{V_n} \cdot \frac{\sin \gamma_{n-2}}{\sin \delta_{n-2}} \sin \beta_{n-1} .$$

With Snell's Law

$$\sin \beta_{n-1} = \frac{V_n}{V_{n-1}} \sin \alpha_{n-1}$$

this yields

$$1/2T_n = q_{n-2}\left(\frac{\sin \phi_{n-2}}{V_{n-1} \cdot \sin \delta_{n-2}} + \frac{\sin \gamma_{n-2}}{V_n \cdot \sin \delta_{n-2}} \quad \frac{V_n}{V_{n-1}} \sin \alpha_{n-1}\right)$$

$$= q_{n-2}\left(\frac{\sin \phi_{n-2}}{V_{n-1} \sin \delta_{n-2}} + \frac{\sin \gamma_{n-2}}{\sin \delta_{n-2}} \quad \frac{\sin \alpha_{n-1}}{V_{n-1}}\right)$$

$$= \frac{q_{n-2}}{V_{n-1}} \left(\frac{\sin \phi_{n-2}}{\sin \delta_{n-2}} + \frac{\sin \gamma_{n-2}}{\sin \delta_{n-2}} \sin \alpha_{n-1}\right)$$

$$= \frac{q_{n-2}}{V_{n-1}} \left(\frac{\sin \phi_{n-2} + \sin \gamma_{n-2} \sin \alpha_{n-1}}{\sin \delta_{n-2}}\right) . \qquad (13)$$

However,

$$\delta_i = \Pi - \gamma_i - \phi_i = \Pi/2 - (\phi_i - \beta_i) .$$

Therefore

$$\sin \delta_{n-2} = \sin(\Pi/2 - (\phi_{n-2} - \beta_{n-2})) = \cos (\phi_{n-2} - \beta_{n-2}) .$$

Also

$$\gamma_i = \Pi/2 - \beta_i$$

hence

$$\sin \gamma_{n-2} = \sin(\Pi/2-\beta_{n-2}) = \cos (\beta_{n-2})$$

Furthermore

$$\beta_{i-1} = \phi_{i-1} + \alpha_i$$

or

$$\alpha_{n-1} = \beta_{n-2} - \phi_{n-2}$$

thus

$$T_{n-1}/2 = \frac{q_{n-2}}{V_{n-1}} \left(\frac{\sin(\beta_{n-2}-\alpha_{n-1}) + \cos(\beta_{n-2}) \sin(\alpha_{n-1})}{\cos(\phi_{n-2}-\beta_{n-2})}\right)$$

$$= \frac{q_{n-2}}{V_{n-1}} \left(\frac{\sin(\beta_{n-2}-\alpha_{n-1}) + \cos(\beta_{n-2}) \sin(\alpha_{n-1})}{\cos(\alpha_{n-1})}\right)$$

or using the formula for the sin of two angles

$$T_n/2 = \frac{q_{n-2}}{V_{n-1}} \left(\frac{\sin\beta_{n-2}\cos\alpha_{n-1}-\sin\alpha_{n-1}\cos\beta_{n-2}+\cos\beta_{n-2}\sin\alpha_{n-1}}{\cos\alpha_{n-1}}\right)$$

$$= \frac{q_{n-2}}{V_{n-1}} \sin\beta_{n-2} \quad . \tag{14}$$

The rest of the proof follows by induction. Assume that for layer i

$$T_i/2 = (q_{i-1}/V_i) \sin \beta_{i-1} \ .$$

Then for layer i-1

$$1/2\Delta t_{i-1} = 1/2(t_{2,i-1} - t_{1,i-1}) = 1/2(\ell_{2,i-1} - \ell_{1,i-1})/V_{i-1} .$$

However,

$$\ell_{2,i-1} - \ell_{1,i-1} = q_{i-2} \frac{\sin \phi_{i-2}}{\sin \delta_{i-2}} .$$

Thus

$$1/2\ t_{i-1} = \frac{q_{i-2}}{V_{i-1}} \frac{\sin \phi_{i-2}}{\sin \delta_{i-2}} .$$

Therefore

$$T_{i-1}/2 = 1/2 \sum_{n=i-1}^{n} \Delta t_j = 1/2\Delta t_{i-1} + 1/2 \sum_{j=i}^{n} \Delta t_j = 1/2(\Delta t_{i-1} + T_i) .$$

Hence

$$T_{i-1}/2 = \frac{q_{i-2}}{V_{i-1}} \frac{\sin \phi_{i-2}}{\sin \delta_{i-2}} + \frac{q_{i-1}}{V_i} \sin \beta_{i-1} .$$

This result along with

$$q_{i-1} = q_{i-2} \frac{\sin \gamma_{n-2}}{\sin \delta_{n-2}}$$

and

$$\sin \beta_{i-1} = \frac{V_i}{V_{i-1}} \sin \alpha_{i-1}$$

and

$$\sin(\phi_{i-2}) = \sin(\beta_{i-2})\cos(\alpha_{i-1}) - \sin(\alpha_{i-1})\cos(\beta_{i-2})$$

$$\sin(\gamma_{i-2}) = \cos(\beta_{i-2})$$

$$\sin(\delta_{i-2}) = \sin(\alpha_{i-1})$$

yields

$$T_{i-1}/2 = \frac{q_{i-2}}{V_{i-2}} \left(\frac{\sin\beta_{i-2}\cos\alpha_{i-1} - \sin\alpha_{i-1}\cos\beta_{i-2} + \cos\beta_{i-2}\sin\alpha_{i-1}}{\cos\alpha_{i-1}}\right).$$

This results in

$$T_{i-1}/2 = \frac{q_{i-2}}{V_{i-1}} \sin \beta_{i-2}$$

or

$$\sin \beta_{i-2} = \frac{T_{i-1}}{2q_{i-2}} V_{i-1} .$$

Therefore for all i such that $i \geq 1$ and $i \leq n$

$$\sin {}_{i-1} = T_i \; V_i/(2q_{i-1}) \; . \qquad (15)$$

This equation, which is known as the time dip equation, will be used to determine the depth of an interface in the next section.

Method of Depth Determination

Using equation 15 with i = 1, it is possible to determine both the position and the dip of the nth interface. To do this, it is necessary to know the travel time to the nth interface, the position of interfaces 1 through n-1, and the velocity of layers 1 through n. In order to determine the position of the nth interface, the following approach is used at several locations along the surface:

1. Calculate $T_1/2$ by subtracting the travel time measured at two adjacent traces and dividing the difference by 2.
2. The result of step 1 is then divided by the distance along the surface between the two traces and multiplied by the velocity of the first layer.
3. Taking the arcsine of the result of step 2 will yield β_o, the angle of inception for a downgoing raypath which will be perpendicular to the nth interface. To locate the nth interface, start tracing the ray at the surface in the direction of β_o. As the interfaces 1 through n-1 are encountered, the raypath is bent according to Snell's Law. It will be necessary to keep track of the travel time as the raypath is traced. Once the raypath has been extended through the (n-1)th interface, it is extended along its final bearing until the total travel time is accounted for. The terminal point of the raypath is then also a point on the nth interface. The interface at this point, will also be perpendicular to the raypath.

By repeating the above three steps at several locations along the surface, it is possible to define the nth interface.

VELOCITY DETERMINATION

In the previous section on depth determination, the accuracy of the result depends upon three things:

1. the accuracy of the model overlying the interface being determined
2. the accuracy of the time picks for this horizon
3. the accuracy of the interval velocity of the final layer being used.

Since the overlying model has already been determined, and the time picks have already been established, the only remaining variable is the interval velocity of the last layer. In many areas there will exist some well control as well as geologic control and possibly even a considerable amount of seismic work. All of these will provide some measure of velocity information which can be used to establish a reasonable estimate of the interval velocity. However in virgin or geologically complex areas, there is still a need for a reasonable estimate of the interval velocity.

Notation

The following notation will be used through this section

v_j ≡ the interval velocity associated with interval j

$\bar{v}_j$ ≡ the stacking velocity associated with the reflection from horizon j.

$T_j \equiv$ the two-way travel time to interface j

$t_j \equiv$ the two-way travel time through layer j

$\theta_1 \equiv$ the dip of the first layer

$V_n \equiv \bar{v}_n \cos\theta_1$

α_i and β_i are defined as in Figure 8

$\nu_i = \nu_{i-1}(v_i/\cos\ _{i-1})\ (\cos\ _{i-1}/v_{i-1})$

$\nu_1 = v_1$.

Initial Interval Velocity Estimation

Since the only known parameters are travel time and stacking velocity, a reasonable approach is to assume that the interval velocity is a function of the stacking velocity. In line with this assumption, Dix in 1955 related interval velocity to stacking velocity for the case of horizontally layered media. His equation is the familiar Dix Interval Velocity Equation

$$v_j^2 = (\bar{v}_j^2 T_j - \bar{v}_{j-1}^2 T_{j-1})/(T_j - T_{j-1}) \ . \qquad (16)$$

Larner (1972) also derived a method of relating interval velocity to stacking velocity. Since Larner was attacking the problem of complex geology, it would be profitable to examine his method here.

Larner's method was adapted from the work of Durbaum (1954). In that paper Durbaum derived an expression for the second derivative of time with respect to offset at the origin in the case of the shotpoint gather. The only variables in the equation were the interval velocities of the various layers and the Snell's Law angles at each interface. Larner was able to prove that this second derivative is identical to the second derivative at the origin in the CDP gather. Using this result, Larner (1972) derived the following equations for the apparent wave speed in the first layer as determined from a reflection off of the nth layer,

$$V_n = \left[\frac{\sum_{j=1}^{n} \nu_j^2 \; t_j}{\sum_{j=1}^{n} t_j} \right]^{1/2} . \qquad (17)$$

Using

$$\nu_n = \nu_{n-1} \, (v_n/\cos\beta_{n-1})(\cos\alpha_{n-1}/v_{n-1})$$

and

$$V_n = \bar{v}_n \cos \theta_1$$

I have rewritten equation 17 as

$$\bar{v}_n^{\,2}\cos^2\theta_1 = \left(\sum_{j=1}^{n-1}\nu_j^{\,2}t_j + v_n^{\,2}\left(\frac{\nu_{n-1}}{\cos\beta_{n-1}}\right)^2\left(\frac{\cos\alpha_{n-1}}{v_{n-1}}\right)^2 t_n\right)\Bigg/\sum_{j=1}^{n}t_j$$

or

$$v_n^{\,2}\left(\frac{\nu_{n-1}}{\cos\beta_{n-1}}\right)^2\left(\frac{\cos\alpha_{n-1}}{v_{n-1}}\right)^2 t_n = \left(\bar{v}_n^{\,2}\cos^2\theta_1\right)\left(\sum_{j=1}^{n}t_j\right) - \left(\sum_{j=1}^{n-1}\nu_j^{\,2}t_j\right).$$

Therefore

$$\frac{v_n^{\,2}}{\cos^2\beta_{n-1}} = \frac{(\bar{v}_n^{\,2}\cos^2\theta_1)(\sum_{j=1}^{n}t_j) - \sum_{j=1}^{n-1}\nu_j^{\,2}t_j}{(\nu_{n-1}/v_{n-1})^2\,(\cos^2\alpha_{n-1})\,t_n}.$$

Substituting from Snell's Law

$$v_n = v_{n-1}\left(\frac{\sin\beta_{n-1}}{\sin\alpha_{n-1}}\right)$$

yields

$$\left(\frac{v^2_{n-1}}{\sin^2\alpha_{n-1}}\right)\left(\frac{\sin^2\beta_{n-1}}{\cos^2\beta_{n-1}}\right) = \frac{(\bar{v}_n^{\,2}\cos^2\theta_1)(\sum_{j=1}^{n}t_j) - \sum_{j=1}^{n-1}\nu_j^{\,2}t_j}{(\nu^2_{n-1})(\cos^2\alpha_{n-1})(t_n)}\,v^2_{n-1}$$

which can be expressed as

$$\tan^2\beta_{n-1} = \frac{(\bar{v}_n^{\,2}\cos^2\theta_1)(\sum_{j=1}^{n}t_j) - (\sum_{j=1}^{n-1}\nu_j^{\,2}t_j)}{(\nu^2_{n-1})(t_n)}\tan^2\alpha_{n-1}. \qquad (18)$$

Knowing β_{n-1} it is possible to calculate v_n from Snell's Law

$$v_n = v_{n-1} \frac{\sin \beta_{n-1}}{\sin \alpha_{n-1}}$$

In order to estimate the interval velocity, a value for β_{n-1} must be calculated. To determine β_{n-1} the following method based upon equation 18 is recommended:

1. Calculate the angle of incidence at the surface (β_o) using the technique outlined in the method of depth determination.
2. Set $\nu_1 = v_1$. Then starting at the surface, extend a ray in the direction of β_o. When the ray intersects the first layer, calculate α_1 and t_1. Then using Snell's Law calculate β_1, then ν_2.
3. Extend the ray down along the path defined by the new β until it intersects the next interface. Calculate t, α, and β for this interface and ν for the next layer.
4. Repeat step 3 for layers 2 through n-2. From interface n-2 extend the ray down along the path defined by β_{n-2} until it intersects interface n-1. Then calculate t_{n-1} and α_{n-1}. Note that β_{n-1} and t_n cannot be obtained since v_n is unknown.
5. Then using equation 18, calculate β_{n-1}. Finally calculate v_n using Snell's Law.

AN ALGORITHM FOR CORRECTING INTERVAL VELOCITY ERROR

Although equation 18 together with Snell's Law seems to solve the problem of determining the interval velocities in structurally complex areas, the equation is only valid at the zero offset position. This presents a problem when related to field data. The problem arises from the fact that for equation 18 to hold for field data the following conditions must be met:

1. No interface may have any appreciable curvature over the range of the CDP gather.
2. The interval velocity of each layer must be constant over the range of the CDP gather.
3. No bed may be terminated laterally either by faulting, or unconformity, or truncation against another horizon.

Because a complex setting will fail to meet at least one if not all of these conditions, equation 18 will not be completely accurate . To overcome this shortcoming, I have developed an algorithm which will correct the error in the interval velocity. The algorithm is derived from equation 17, and involves setting ν_1 equal to v_1. This along with the definition for ν_2:

$$\nu_2 = \nu_1(v_2/\cos\beta_1)/v_1/\cos\alpha_1)$$

yields

$$\nu_2 = v_1(v_2/\cos\beta_1)/(v_1/\cos\alpha_1) = v_2 \cos\alpha_1/\cos\beta_1 .$$

And for ν_3

$$\nu_3 = \nu_2(v_3/\cos\beta_2)(v_2\cos\alpha_2) = v_2 \frac{\cos\alpha_1}{\cos\beta_1} \frac{v_3}{v_2} \frac{\cos\alpha_2}{\cos\beta_2}$$

$$= v_3\left(\frac{\cos\alpha_1}{\cos\beta_1}\right) \left(\frac{\cos\alpha_2}{\cos\beta_2}\right) .$$

Thus it can be proved by induction that

$$\nu_n = v_n \prod_{i=1}^{n-1} \left(\frac{\cos \alpha_i}{\cos \beta_i}\right) . \quad (19)$$

Substituting equation 19 into equation 17 yields

$$V_n^2 = \left(\sum_{j=2}^{n} v_j^2 \left[\prod_{i=1}^{j-1} \left(\frac{\cos \alpha_i}{\cos \beta_i}\right)^2 \right] t_j + v_1 t_1 \right) \Big/ \sum_{j=1}^{n} t_j$$

which along with $V_n = \bar{v}_n \cos \theta_1$ results in

$$\bar{v}_n^2 (\cos^2\theta_1)(\sum_{j=1}^{n} t_j) = \sum_{j=2}^{n} v_j^2 (\sum_{i=1}^{j-1} \frac{\cos\alpha_i}{\cos\beta_i})^2 t_j + v_1^2 t_1$$

Rearranging terms gives the result

$$v_n^2 (\sum_{i=1}^{n-1} \frac{\cos^2\alpha_i}{\cos^2\beta_i}) t_n = (\bar{v}_n^2 \cos^2\theta_i)(\sum_{j=1}^{n} t_j) - \sum_{j=2}^{n-1} \left[v_j^2 (\prod_{i=1}^{j-1} \frac{\cos\alpha_i}{\cos\beta_i})^2 t_j \right] - v_1^2 t_1 . \quad (20)$$

However from the section on depth determination, the angles β_i for i equal to 1 through n-2, and the angles α_i for i equal to 1 through n-1 are all known. Also the values of v_i for i equal to 1 through n-1 have already been determined, as have all the values of t_i. Therefore with the following abbreviations

$$c_1 = (\cos^2\alpha_{n-1}) \prod_{i=1}^{n-2} \left(\frac{\cos\ \alpha_i}{\cos\ \beta_i}\right)^2 t_n$$

$$c_2 = \left(\sum_{j=1}^{n} t_j\right) \cos^2\ \theta_1$$

$$c_3 = \sum_{j=2}^{n-1} \left[v_j^{\ 2} \left(\prod_{i=1}^{j-1} \frac{\cos\alpha_i}{\cos\beta_i}\right)^2 t_j\right] + v_1^{\ 2} t_1$$

equation 20 can be rewritten as

$$(v_n^{\ 2}/\cos^2\beta_{n-1})\ c_1 = \bar{v}_n^{\ 2}\ c_2 - c_3.$$

Multiplying by $\cos^2\beta_{n-1}$ gives

$$c_1\ v_n^{\ 2} = c_2\ \bar{v}_n^{\ 2}\ \cos^2\beta_{n-1} - c_3\ \cos^2\beta_{n-1}.$$

Treating v_n, $\bar{v}_n$, and β_{n-1} as three independent variables and taking differentials yields

$$2c_1 v_n dv_n = 2c_2\bar{v}_n\cos^2\beta_{n-1}d\bar{v}_n - c_2\bar{v}_n^{\ 2}\sin\beta_{n-1}\cos\beta_{n-1}d\beta_{n-1} + c_3$$
$$\sin\beta_{n-1}\cos\beta_{n-1}d\beta_{n-1}$$

or

$$c_1 v_n dv_n = c_2 \bar{v}_n \cos\beta_{n-1} d\bar{v}_n + \frac{c_3 - c_2 \bar{v}_n^{\,2}}{2} \sin\beta_{n-1} \cos\beta_{n-1} d\beta_{n-1}. \quad (21)$$

In order to simplify equation 21, $d\beta_{n-1}$ is assumed to be negligible for small values of dv_n and $d\bar{v}_n$. This assumption follows from Snell's Law and implies that $\cos\beta_{n-1}$ will be constant for small changes in v_n and $\bar{v}_n$. Therefore equation 21 can be written as

$$c_1 \cdot v_n \cdot dv_n = c_4 \cdot \bar{v}_n \cdot d\bar{v}_n$$

where

$$c_4 = c_2 \cos\beta_{n-1} .$$

Rearranging terms yields

$$dv_n = k \frac{\bar{v}_n}{v_n} d\bar{v}_n \quad (22)$$

where

$$k = \frac{\sum_{j=1}^{n} t_j \cos^2\theta_i \cos\beta_{n-1}}{\cos\alpha_{n-1} \prod_{i=1}^{n-2} \frac{\cos\alpha_i}{\cos\beta_i} t_n} = \left(\frac{\sum_{i=1}^{n} t_i}{t_n} \right) \left(\prod_{i=1}^{n-1} \frac{\cos\beta_i}{\cos\alpha_i}^{2} \right) \cos^2\theta_1 .$$

Unfortunately little can be said about the range of values of k other than that k will always be positive. An examination of the individual factors in k will serve to demonstrate both the problem and that k is greater than zero. Since each t_i is positive, the first factor is greater than one. If $v_{i+1} > v_i$, as is usually the case, then $\beta_i > \alpha_i$ and $\cos\beta_i < \cos\alpha_i$. Therefore $\cos\beta_i/\cos\alpha_i$ will be less than 1 and thus $\prod_{i=1}^{n-1} (\cos\beta_i/\cos\alpha_i)$ will be less than 1. Also since β_i will always be less than 90 degrees, and greater than -90 degrees, $\cos\beta_i$ will always be greater than zero. The same argument holds for α_i. This means that $\cos\beta_i/\cos\alpha_i$ will always be greater than zero. Therefore, $\prod_{i=1}^{n-1} (\cos\beta_i/\cos\alpha_i)$ will usually be less than one and it will always be greater than zero. The final term, $\cos^2\theta_1$, will always be positive and less than one. Therefore, since all three terms are positive, their product, k, must also be positive. However, since the first term is always greater than one, the second is usually less than one, and the third is always less than one, little more may be said about the product of the three.

Since there is no simple method for determining k, an iteration method for determining the interval velocity for the last layer and for determining k will be used. First by rewriting equation 22 as

$$k = \frac{v_n}{\bar{v}_n} \frac{d\, v_n}{d\, \bar{v}_n} \tag{23}$$

one observes that one is a reasonable approximation of k.

Therefore it is possible to approximate the value of Δv_n by

$$\Delta v_n = \frac{\bar{v}_n}{v_n} \Delta \bar{v}_n \ . \tag{24}$$

Here $\Delta \bar{v}_n$ is the difference between the stacking velocity from the field data and the stacking velocity associated with the selected interval velocity for the current model. The values of v_n and $\bar{v}_n$ are supplied by performing offset raytracing on that model. For the next model one uses the current model to compute a new k according to

$$k = \frac{v_n}{\bar{v}_n} \frac{\Delta v_n}{\Delta \bar{v}_n} \tag{25}$$

and repeats the process.

RESULTS

The results of using the above approach on the overthrust model data (i.e. Figure 1 and again in Figures 11 and 12) are very good. These results are shown in Figure 13 and in Table 1. Table 1 is a comparison of the true interval velocities from the model with the average interval velocities from the program. The calculated velocities are in all cases within 10% of the true velocities. Figure 13 is the cross section produced by the program. This cross section is developed iteratively by the depth determination section of the program. Again there is a good correlation between the model and the cross section generated by the program.

To provide a comparison with another approach, the same data were run through a program which was based on the paper by Larner and Rooney (1972). This method was chosen because it is purported to handle complex geologic structures. The resulting cross section is displayed in Figure 14. This figure illustrates the shortcomings of the analytical method. In this figures, the shallower horizons have been reasonably defined. However the shallow events which terminate laterally introduce errors which propagate into the deeper horizons and result in the anticline on horizon 16 and the exaggerated structure on horizon 15.

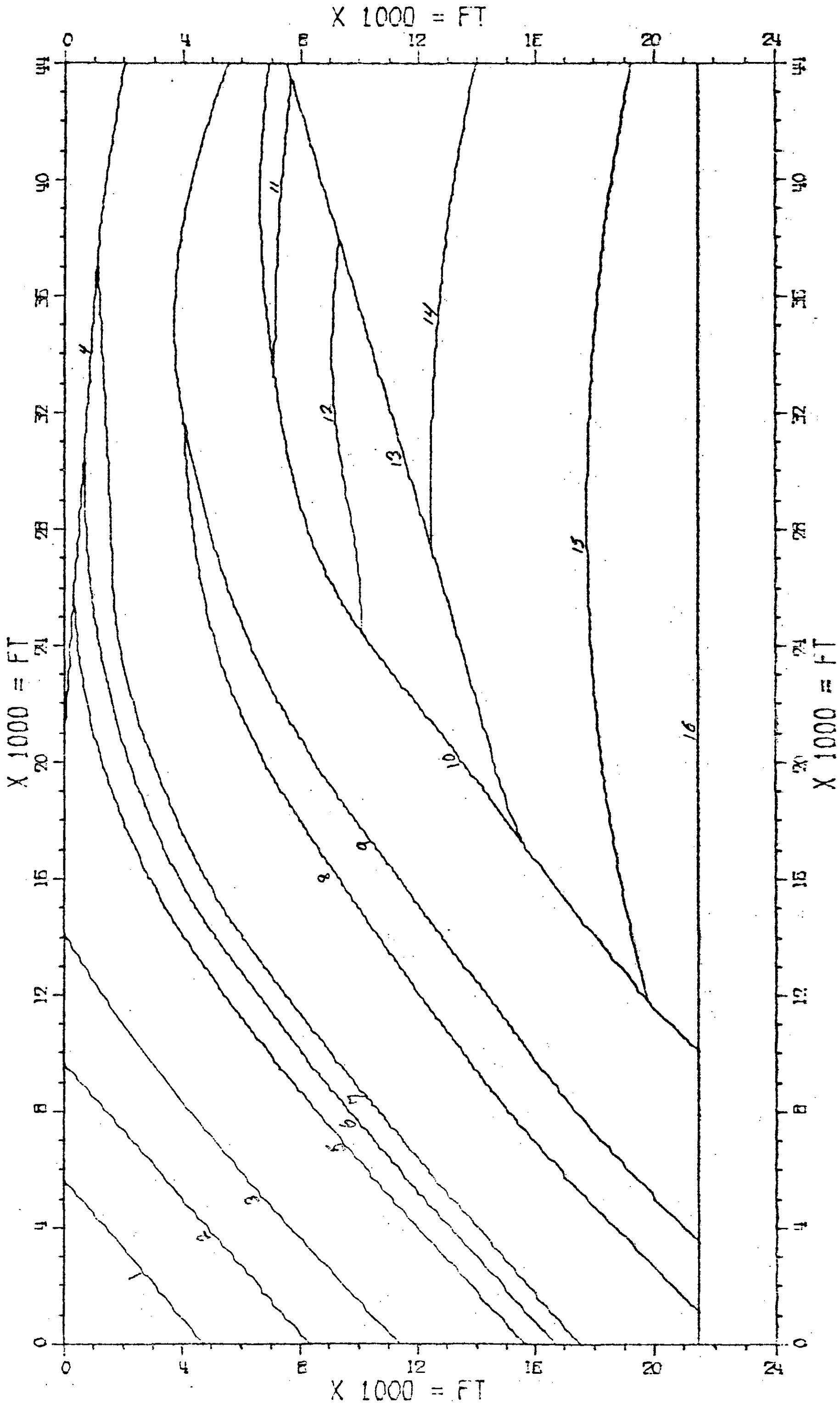

A Geologic Model of the Overthrust Belt

FIGURE 11

Picked Seismic Reflection Events from the Overthrust Model

FIGURE 12

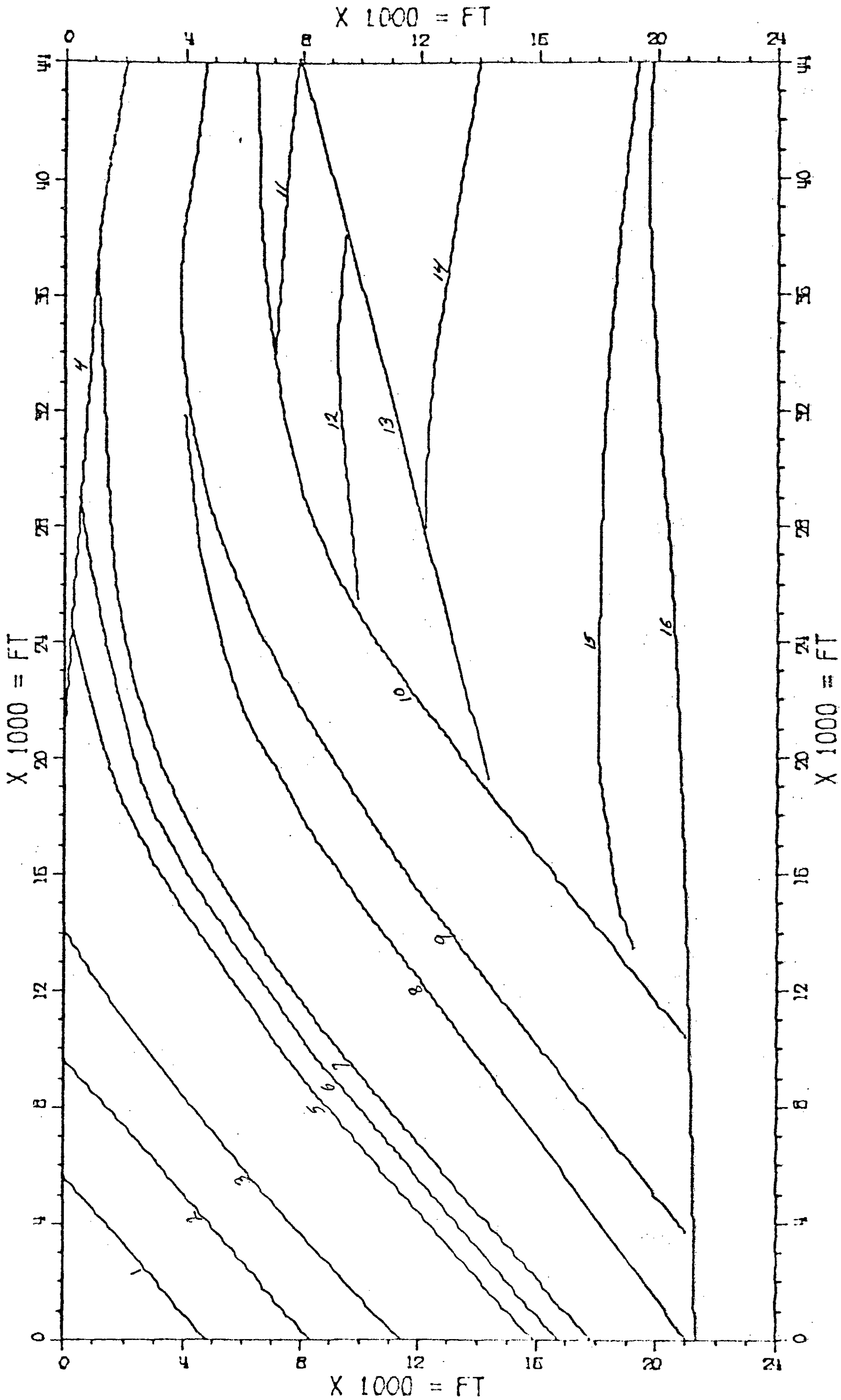

Computer Generated Model

FIGURE 13

TABLE 1

Comparison of Model Velocities and Calculated Velocities

LAYER	MODEL VELOCITY	AVERAGE CALCULATED VELOCITY
5	12100	11785
6	15875	15291
7	14000	14243
8	17900	18472
9	19000	19086
10	18524	18493
11	18000	17000
12	19000	19082
13	19100	17897
14	13000	13170
15	15600	16231
16	18000	19120

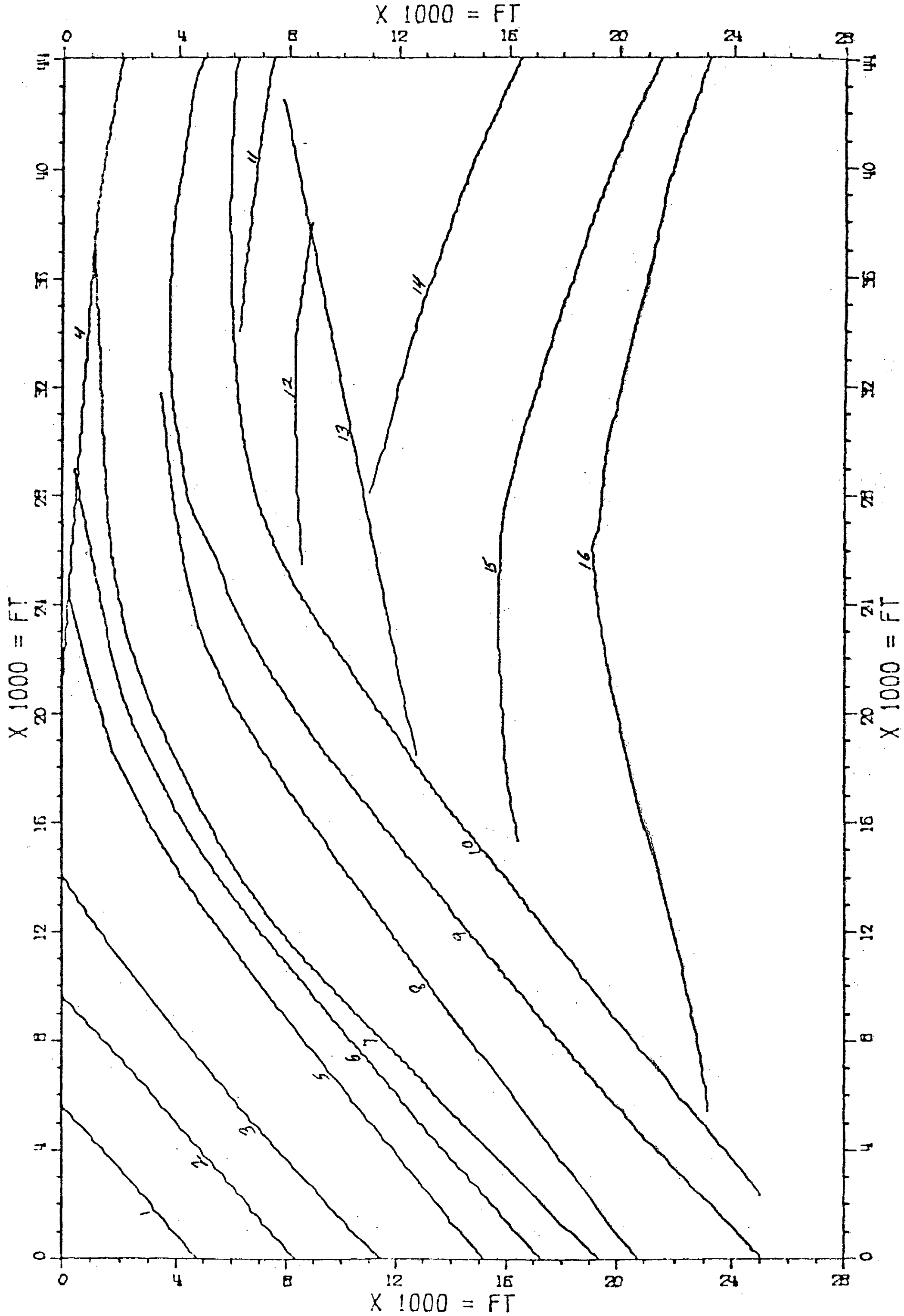

Model Generated by the Analytic Method

FIGURE 14

In Table 2, the average interval velocity for each layer derived by the analytical method is compared with the true interval velocity and with the average interval velocity derived from the method outlined in this paper, the CDP method. In this table several of the interval velocities from the analytical method are not even reasonably close to the true interval velocities. Thus the analytical approach is unable to handle all of the problems which are presented by complex geology.

The data used by the program were obtained by performing offset raytracing on the overthrust model. A horizontal velocity analysis was then performed on the results of the raytracing. The results of the horizontal velocity analysis were interpreted, and then the interpreted velocities and associated time picks were fed into the depth determination program. Approximately ten hours of CPU time were required to run the data from the overthrust model through the depth determination program. The program was written in Algol, and the machine used to run it is the B-6800. Although ten hours were required for the total run, the time spent on each layer varied from 10 minutes to 2 1/2 hours.

The difference in run time for each layer is caused by the length of the layer being determined, the number of intervening layers between a given layer and the surface,

TABLE 2

Comparison of Interval Velocities

LAYER	MODEL VELOCITY	ANALYTICAL METHOD	CDP METHOD
5	12100	11080	11785
6	15875	15023	15291
7	14000	13790	14243
8	17900	14314	18472
9	19000	17563	19086
10	18524	13764	18493
11	18000	17909	17000
12	19000	20722	19082
13	19100	18877	17897
14	13000	17571	13170
15	15600	13913	16231
16	18000	17142	19120

and the complexity of the overlying geology. The length of the layer determines the number of CDP's that must be traced along the layer. As the length of the layer increases, more CDP's are required and therefore more time will be required. Because the program must determine the location of the point where each leg of the raypath intersects each intervening layer, more time will be required for the deeper layers. The complexity of the geology introduces errors into the equation used to obtain a first approximation of the interval velocity. This in turn requires more iterations to establish the correct interval velocity.

The number of points used to define each horizon will also effect the run time. The reason is that in order to determine the point of intersection between a ray and a given horizon, each segment along the horizon must be checked. Therefore the fewer the points, the smaller the number of segments, and thus less run time. However, in order to demonstrate the accuracy of the method, the only user intervention in the example was in specifying the location of the CDP's for offset raytracing. Since the program usually overdefines each horizon, the lack of user intervention results in a very large number of points being used to automatically define each horizon. It is therefore recommended that the user intervene after the program has determined two or three layers, and redefine the horizons to both smooth the horizons and to reduce the number of points used.

Because small perturbations in an interface can propagate into the underlying layers with an increasing effect, it is necessary to implement a smoothing routine which will remove any perturbations which occur along an interface. In this way small errors in time will be smoothed out along with any propagation errors and roundoff errors.

CONCLUSIONS

The algorithm does provide a means of determining interval velocities as well as migrated depth in areas of complex geology. Furthermore the method requires no special data or equipment as only the travel time and stacking velocities are needed as input. Although this approach does an excellent job in complex areas, because of the computer time involved, it is not recommended in locations where other methods, such as Dix's or Larner's will also yield acceptable results. In those areas where nothing else works, this method should yield an acceptable answer. Also if some limits on the interval velocities are known, these can be used as bounds for the iteration scheme. If the velocities are known from well logs for example, this information can be input into the depth determination scheme to obtain a cross section.

The algorithm presented in this paper will allow the interval velocity for a given layer to vary across the model. This occurs because the interval velocity is calculated at each CDP independently of the neighboring CDP's, thus allowing the interval velocity to vary from one CDP to the next.

Since the method is an extension of raytracing, it should be adaptable to any offset raytracing program. It is therefore possible to program this method for any of the mini-computers used by the seismic industry. Because this approach can be put on a mini-computer it need not be a part of a research organization, but can be accessible to the field geophysicist.

The method presented in this paper provides an accurate, flexible, and easy-to-use means of calculating interval velocities and geologic depths in structurally complex areas. It would be a valuable addition to any seismic interpretation package.

Naturally, this method will become more practical in all cases if the cost of computing continues to decrease.

APPENDIX A

Calculation of Least Squares Velocity Curve

The hyperbolic moveout equation is

$$T_x^2 = T_o^2 + X^2/\bar{v}^2$$

where

X is the offset,

$\bar{v}$ is the stacking velocity,

T_o is the travel time at zero offset,

T_x is the travel time at an offset of X.

Using CDP raytracing it is possible to obtain several sets of values for T_x and X. With several sets of data, all that remains is to determine a best fit hyperbola through the data. To calculate the hyperbola, the moveout equation must be rewritten as

$$T_x^2 = T2 + X^2 * S2 \ .$$

Here $T2 = T_o^2$ and $S2 = 1/\bar{v}^2$. This is done in order to simplify the mathematics later on. The error between the raytracing data and the hyperbola can then be expressed as

$$e_i = Y_i^2 - T_{xi}^2$$

or

$$e_i = Y_i^2 - T2 - X_i^2 * S2$$

where

e_i is the error measured at trace i,

Y_i is the time on trace i obtained from raytracing,

X_i is the offset for trace i.

The least squares error equation is then determined by summing the error for all trace and squaring the result. Then derivatives are taken with respect to the coefficients. The resulting equations are set equal to zero. This will produce the matrix equation

$$\begin{pmatrix} n & \sum_{i=1}^{n} X_i^2 \\ \sum_{i=1}^{n} X_i^2 & \sum_{i=1}^{n} X_i^4 \end{pmatrix} \begin{pmatrix} T2 \\ S2 \end{pmatrix} = \begin{pmatrix} \sum_{i=1}^{n} Y_i^2 \\ \sum_{i=1}^{n} X_i^2 \; Y_i^2 \end{pmatrix} .$$

The equation is then solved for T2 and S2. The values of T_o and $\bar{v}$ are determined from

$$T_o = (T2)^{1/2}$$

$$\bar{v} = (1/S2)^{1/2} .$$

APPENDIX B

Sattleger's Approach

Sattleger in 1964 presented a method that would define the location of a desired interface as well as the interval velocity of the layer above the interface. The ensuing proof parallels the work of Sattleger and will use the following definitions:

t_j ≡ the observed travel time between the shotpoint and the geophone j

z_n ≡ the thickness of layer n under the shotpoint

θ_n ≡ the dip of interface n

v_n ≡ the interval velocity of layer n

z_n' ≡ an approximation of z_n

θ_n' ≡ an approximation of θ_n

v_n' ≡ an approximation of v_n

ε_j ≡ the difference between the travel time calculated from a model and the measured travel time t_j.

Sattleger's approach is recursive and it is first assumed that the thickness, dip, and interval velocity for layers 1 through n-1 are known for all points of the model. Therefore only those parameters which relate to layer n are considered in the proof. In his proof, Sattleger represents the travel time to each geophone j plus a correction term as a function of the unknowns z_n, θ_n, and v_n

$$t_j + \varepsilon_j = f_j(z_n, \theta_n, v_n)$$

Where f_j is obtained by offset raytracing. Here the objective is to minimize the ε_j's. It is then assumed that approximate values for the unknowns are available. The unknowns could then be represented by

$$z_n = z_n' + \Delta z_n$$
$$\theta_n = \theta_n' + \Delta\theta_n \qquad (2)$$
$$v_n = v_n' + \Delta v_n.$$

Sattleger then rewrites equation 1 as

$$t_j+\varepsilon_j = \frac{\partial f_j}{\partial z_n} \Delta z_n + \frac{\partial f_j}{\partial \theta_n} \Delta\theta_n + \frac{\partial f_j}{\partial v_n} \Delta v_n + f_j(z_n', \theta_n', v_n') \qquad (3)$$

where $j = 1,2...,m$ and m is the number of geophones. At this point, he states that none of the terms $f_j(z_n', \theta_n', v_n')$ $\frac{\partial f_j}{\partial z_n}$, $\frac{\partial f_j}{\partial \theta_n}$, $\frac{\partial f_j}{\partial v_n}$ are known, nor can the functions be determined. To get around this difficulty, he proposed to perform offset raytracing using the following seven sets of parameters in the models:

$$(z_n' \quad , \theta_n' \quad , v_n' \quad)$$
$$(z_n'-\Delta z_n , \theta_n' \quad , v_n' \quad)$$

$$
\begin{array}{llll}
(z_n'+\Delta z_n , & \theta_n' , & v_n' &) \\
(z_n' , & \theta_n'-\Delta\theta_n , & v_n' &) \\
(z_n' , & \theta_n'+\Delta\theta_n , & v_n' &) \\
(z_n' , & \theta_n' , & v_n'-\Delta v_n &) \\
(z_n' , & \theta_n' , & v_n'+\Delta v_n &)
\end{array} \tag{4}
$$

This provides values for $f_j(z_n',\theta_n',v_n')$, $f_j(z_n'-\Delta z_n,\theta_n,v_n)$, ..., $f_j(z_n',\theta_n',v_n'+\Delta v_n)$ and thus the differential quotients are approximated using

$$
\begin{aligned}
\frac{\partial f_j}{\partial z_n} &\approx a_j = [f_j(z_n'+\Delta z_n, \theta_n', v_n')-f_j(z_n'-\Delta z_n,\theta_n,v_n)]/(2\Delta z_n) \\
\frac{\partial f_j}{\partial \theta_n} &\approx b_j = [f_j(z_n',\theta_n'+\Delta\theta_n,v_n')-f_j(z_n',\theta_n'-\Delta\theta_n,v_n)]/(2\Delta\theta_n) \\
\frac{\partial f_j}{\partial v_n} &\approx c_j = [f_j(z_n',\theta_n',v_n'+\Delta v_n)-f_j(z_n',\theta_n',v_n'-\Delta v_n)]/(2\Delta v_n) .
\end{aligned} \tag{5}
$$

Using

$$\ell_j = t_j - f_j(z_n',\theta_n',v_n') \tag{6}$$

for simplicity, equation 3 is rewritten as

$$\varepsilon_j = a_j \; \Delta z_n + b_j \; \Delta\theta_n + c_j \; \Delta v_n - \ell_j \tag{7}$$

Using least squares analysis he derives the following equation

$$\begin{pmatrix} \Sigma a_j^{\,2} , & \Sigma a_j b_j , & \Sigma a_j c_j \\ \Sigma a_j b_j , & \Sigma b_j^{\,2} , & \Sigma b_j c_j \\ \Sigma a_j c_j , & \Sigma b_j c_j , & \Sigma c_j^{\,2} \end{pmatrix} \begin{pmatrix} \Delta z_n \\ \Delta \theta_n \\ \Delta v_n \end{pmatrix} = \begin{pmatrix} \Sigma a_j \ell_j \\ \Sigma b_j \ell_j \\ \Sigma c_j \ell_j \end{pmatrix} . \qquad (8)$$

This equation is used to solve for $\Delta z_n, \Delta\theta_n$, and Δv_n. These terms are then used to calculate either z_n, θ_n, and v_n, or if the error is still too large, new values of z_n', θ_n', and v_n'. Although this method will accurately define a given interval, it has the drawback of requiring large amounts of computer time for a single layer. Most of the computer time is taken in raytracing seven different models for each iteration.

SELECTED BIBLIOGRAPHY

Al-Chalabi, M., 1973, "Series approximation in velocity and travel time computation", Geophysical Prospecting, v. 21, p. 783-795.

Al-Chalabi, M., 1974, "An analysis of stacking, rms, average, and interval velocities over a horizontally layered ground", Geophysical Prospecting, v. 22, p. 458-475.

Bortfeld, R., 1957, "A method of dip corrections for expanding spread velocity measurements", Geophysica Pura e Applicata, v. 38, p. 32-44.

Dix, E. H., 1955, "Seismic velocities from surface measurements", Geophysics, v. 20, p. 68-86.

Durbaum, H., 1953, "Possibilities of constructing true raypaths in reflection seismic interpretation", Geophysical Prospecting, v. 1, p. 125-139.

Durbaum, H., 1954, "Zur bestimmung von wellengeschindigkeiten aus reflexionsseimischen messungen", Geophysical Prospecting, v. 2, p. 151-167.

Everett, J. E., 1974, "Obtaining interval velocities from stacking velocities when dipping horizons are included", Geophysical Prospecting, v. 22, p. 122-142.

Gardner, G. H. F., French, W. S., and Matzak, T., 1974, "Elements of migration and velocity analysis", Geophysics, v. 39, p. 811-825.

Gerritsma, P. H. A., 1977, "Time-to-depth conversion in the presence of structure", Geophysics, v. 42, p. 760-772.

Hubral, Peter, 1975, "Locating diffractor below plane layers of constant interval velocity and varying dip", Geophysical Prospecting, v. 23, p. 313-322.

Hubral, Peter, 1976, "Interval velocities from surface measurements in the three-dimensional plane layer case", Geophysics, v. 41, p. 233-242.

Hubral, Peter, 1976, "CDP ray modeling in the presence of 3-D plane isovelocity layers of varying dip and strike", Geophysical Prospecting, v. 24, p. 478-491.

Larner, K. L. and M. Rooney, 1972, "Interval velocity computation for plane dipping multi-layered media", Forty-second Annual S.E.G. Convention.

Levin, F. K., 1971, "Apparent velocity from dipping interface reflections", Geophysics, v. 36, p. 510-516.

McCaslin, John C., 1974, "Interest swells in overthrust belt campaign", Oil and Gas Journal, v. 72, no. 36, p. 162-163.

-----, 1976, "Exploration flares along Rockies overthrust belt", Oil and Gas Journal", v. 74, no. 50, p. 23-27.

Krey, Th., 1976, "Computation of interval velocity from CDP moveout times for n layers with arbitrary dips and curvatures in three dimensions, when assuming small shot-geophone distances", Geophysical Prospecting, v. 24, p. 52-71.

Sattleger, J., 1965, "A method of computing time interval velocities from expanding spread data in the case of arbitrary long spreads and arbitrarily dipping plane interfaces", Geophysical Prospecting, v. 13, p. 306-318.

Shah, Parvin M., 1973, "Use of wavefront curvature to relate seismic data with subsurface parameters", Geophysics, v. 38, p. 812-825.